Detection and Quantification through a Lipid Membrane Using the Molecularly Controlled Semiconductor Resistor

ARTICLE *in* LANGMUIR · NOVEMBER 2011

Impact Factor: 4.46 · DOI: 10.1021/la203502b · Source: PubMed

8 AUTHORS, INCLUDING:

Hubert Marek Piwoński
King Abdullah University of Science and Tec…
9 PUBLICATIONS **126** CITATIONS
SEE PROFILE

Eyal Capua
Weizmann Institute of Science
8 PUBLICATIONS **50** CITATIONS
SEE PROFILE

Gilad Haran
Weizmann Institute of Science
85 PUBLICATIONS **4,039** CITATIONS
SEE PROFILE

Ron Naaman
Weizmann Institute of Science
304 PUBLICATIONS **5,425** CITATIONS
SEE PROFILE

Langmuir

ARTICLE

pubs.acs.org/Langmuir

Detection and Quantification through a Lipid Membrane Using the Molecularly Controlled Semiconductor Resistor

Danny Bavli,[§] Maria Tkachev,[§] Hubert Piwonski, Eyal Capua, Ian de Albuquerque, David Bensimon,[†,‡] Gilad Haran, and Ron Naaman*

Department of Chemical Physics, Weizmann Institute of Science, Rehovot, 76100, Israel

[†]LPS-ENS, CNRS UMR8550, 24 rue Lhomond, Paris 75005 France

[‡]Department of Chemistry and Biochemistry, University of California, Los Angeles, California, United States

Supporting Information

ABSTRACT: The detection of covalent and noncovalent binding events between molecules and biomembranes is a fundamental goal of contemporary biochemistry and analytical chemistry. Currently, such studies are performed routinely using fluorescence methods, surface-plasmon resonance spectroscopy, and electrochemical methods. However, there is still a need for novel sensitive miniaturizable detection methods where the sample does not have to be transferred to the sensor, but the sensor can be brought into contact with the sample studied. We present a novel approach for detection and quantification of processes occurring on the surface of a lipid bilayer membrane, by monitoring the current change through the n-type GaAs-based molecularly controlled semiconductor resistor (MOCSER), on which the membrane is adsorbed. Since GaAs is susceptible to etching in an aqueous environment, a protective thin film of methoxysilane was deposited on the device. The system was found to be sensitive enough to allow monitoring changes in pH and in the concentration of amino acids in aqueous solution on top of the membrane. When biotinylated lipids were incorporated into the membrane, it was possible to monitor the binding of streptavidin or avidin. The device modified with biotin-streptavidin complex was capable of detecting the binding of streptavidin antibodies to immobilized streptavidin with high sensitivity and selectivity. The response depends on the charge on the analyte. These results open the way to facile electrical detection of protein−membrane interactions.

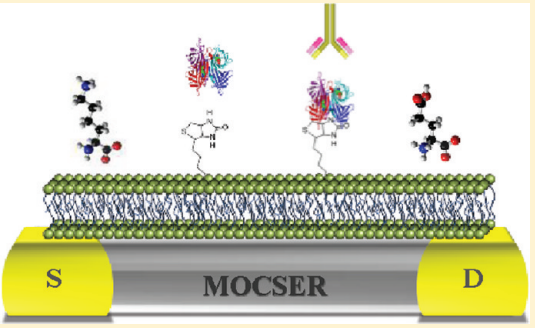

INTRODUCTION

The detection of covalent and noncovalent binding events between molecules and biomembranes is a fundamental goal of contemporary biochemistry and analytical chemistry. This detection serves for the basic study of central biological processes like signaling, and for the development of high throughput screening of drug candidates from large libraries of molecules that potentially recognize a specific membrane receptor. Currently, such studies are performed routinely using fluorescence methods,[1] surface-plasmon resonance spectroscopy,[2] and electrochemical methods.[3−9] However, there is still need for novel sensitive miniaturizable detection methods, e.g., for point-of-care testing. Here, we report on the application of a transistor-like device, the molecularly controlled semiconductor resistor (MOCSER),[10] as a means for monitoring processes occurring on a membrane and the interaction of proteins in solution with proteins embedded within or connected to the membrane.

We investigated phospholipid supported bilayers as a model membrane. Supported phospholipid bilayers are well-known biomimetic systems, similar in physical and chemical properties to natural cell membranes.[11] The potential to use artificial lipid membranes for studying cell-membrane functions was demonstrated by Mueller et al.[12] Applicability of these membranes for monitoring enzyme−substrate and antigen−antibody interactions was verified almost half a century ago.[13]

The preparation and characterization of model membranes on solid supports (e.g., semiconductors) is a practical and scientifically important research area.[14] Practical applications include smart biosensor devices for studying basic membrane processes and membrane−analyte interactions, as well as other biotechnological applications.[15−18]

Recent advances in microelectronics and nanotechnology, improvement in sensor function, and emergence of new types of biosensors have increased the interest in development of lipid membrane-based systems. Electrochemical methods were applied since they allow direct conversion of biological information to electronic signal. They are well suited for investigation of biomembrane functions due to their operation simplicity, low cost, and capability of real-time measurements. Typically, electrochemical biosensors employ amperometric, potentiometric, or impedimetric transducers.[3−9]

In the present work, the transmission of information through a bilayer membrane does not involve charge/mass transfer, but

Received: September 6, 2011
Revised: November 15, 2011
Published: November 29, 2011

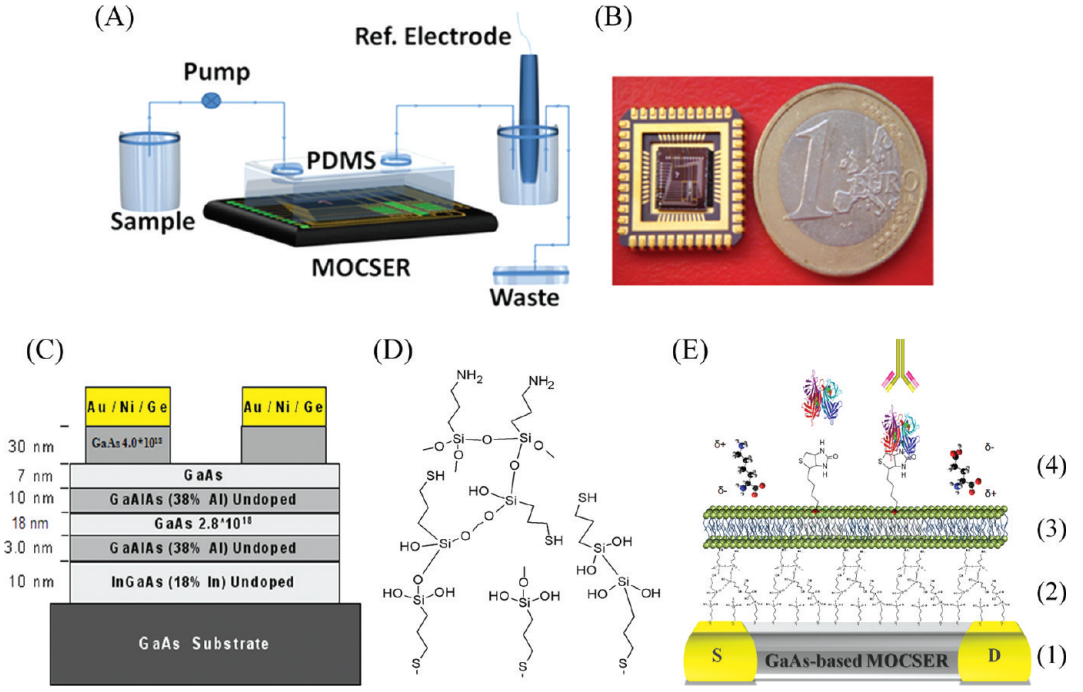

Figure 1. (A) Schematic representation of the experimental setup. A peristaltic pump was used to transfer analyte samples to a GaAs-based MOCSER on top of which a PDMS-based flow cell was constructed. An Ag/AgCl reference electrode was connected via a salt bridge. (B) All electrical measurements were performed with wire bonded devices. The die contained 16 devices from which 4 were selected and measured simultaneously. (C) Schematic representation of the GaAs pseudomorphic high electron mobility transistor (pHEMT) structure used for device fabrication. (D) Schematic picture of the MPS and APS layers. (E) The GaAs-device (1) was coated with (3-mercaptopropyl)-trimethoxysilane (MPS) layer and (3-aminopropyl)-trimthoxysilane (APS) (2), on top of which a lipid bilayer membrane was formed (3), and interactions with various analytes (4) were investigated.

rather relies on the ability of adsorbed organic molecules to control electronic devices.[19−21] In this hybrid approach, molecular functionality is utilized to influence the electronic properties of the device. The interaction between the dipoles of the adsorbed molecules and the semiconductor surface modifies electrical potential at the interface by changing distribution of electronic surface states and the net surface-charge density.[22−24] Incorporating biologically active molecules into the adsorbed membrane allows direct measurement of the electric effect caused by interaction of these molecules with analyte species. In this way, intrinsic molecular properties are translated into measurable electrical signals.

Sensors based on field-effect transistor (FET) configuration have been utilized since the early 1970s.[25,26] This special class of sensors make use of the potentiometric effect at a gate electrode.[27] Currently, biosensing applications focus on ion-selective FET (ISFET or CHEMFET) devices. In ISFET, the regular gate is placed in a liquid electrolyte, and the diffusion of specific analytes toward the electrode can be controlled by insertion of a selective membrane positioned on the gate. ISFET approach was utilized, for example, for studying enzyme−substrate recognition and for detecting neurons or living cell activity.[28−32] A theoretical model for biorecognition of acetylcholine applying enzyme-modified ISFET was provided recently.[33] According to this model, the electrical response of the device, during enzyme−substrate recognition events, depends on cooperative effects of local pH changes and molecular dipole variations.

In contrast to ISFET, the MOCSER, applied in the present study, represents a resistor rather than transistor, since it does not incorporate any gate electrode. Its operation is based on variation in the electrochemical potential on the surface of a GaAs-based device itself, which is similar in structure to FET, but instead of a gate electrode, the area between the source and the drain is covered by chemically adsorbed molecules.[34,35] Monitoring the current through the device allows detection of surface potential changes resulting from the interaction of the analyte molecules with the molecules adsorbed on the device. The sensitivity of the MOCSER is achieved by applying GaAs based pseudomorphic high electron mobility transistor (pHEMT) configuration. The conducting channel of these devices is a very thin layer of highly mobile conducting electrons (a two-dimensional electron gas) and its conductivity is highly sensitive to changes in surface potential. In the past, MOCSER was applied for sensing a large variation of species both in the gas phase[36,37] and in liquids.[38,39]

We evaluated the applicability of the MOCSER to sense an analyte through a bilayer membrane formed on the device surface. Because of the new experimental concept applied here, we provide a detailed description of the methods used for preparing the sensing devices and specifically the characterization of the membrane deposited. In the Results section, we introduce several applications, including pH sensing, sensing of either positively or negatively charged amino acids, sensing of interaction between avidin or streptavidin in solution and biotin embedded within a membrane, and sensing the interaction of rabbit and mouse antibodies for streptavidin with streptavidin attached to biotinylated membrane. The results are followed by a discussion of the mechanism by which the MOCSER reacts to all these analytes, and of future prospects.

MATERIALS AND METHODS

MOCSER Fabrication. Figure 1 shows the device used and the experimental setup. The GaAs/AlGaAs-based device is a pseudomorphic high-electron-mobility transistor with a 600 μm long and 200 μm wide

dx.doi.org/10.1021/la203502b |*Langmuir* 2012, 28, 1020–1028

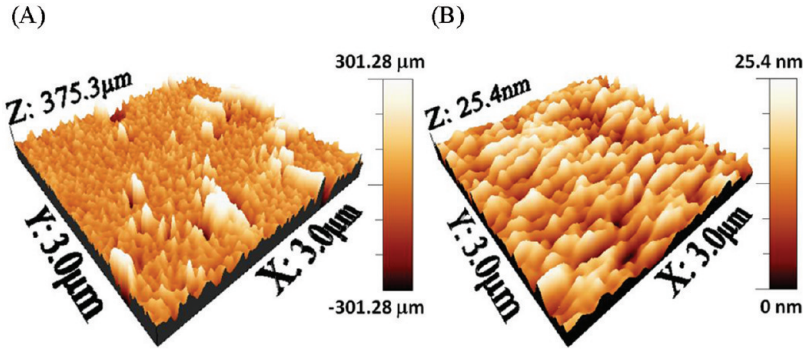

Figure 2. AFM images showing the effect of water exposure on a bare GaAs surface (A) and on a surface covered by ~25-nm MPS (B). Note that the height scale in (A) is in μm while in (B) it is in nm.

conducting channel. Each fabricated die contains 16 devices from which 4 were selected and measured simultaneously in each experiment.

Since GaAs is used in an aqueous environment where it is susceptible to etching, a protective layer of (3-mercaptopropyl)-trimethoxysilane (MPS) was fabricated on top of each device according to a common procedure.[40] The MPS layer thickness was determined by ellipsometry to be in the range of 25−30 nm. The protection against etching provided by this layer was evaluated by atomic force microscopy (AFM) on GaAs samples that were immersed in doubly distilled water (DDW) for 24 h. AFM images were acquired using the tapping mode in DDW at room temperature (23−25 °C). Following the immersion in water, there is a clear difference between the highly etched surface of bare GaAs (Figure 2A) and the sample protected by the MPS layer (Figure 2B).

It is important to appreciate that coating the GaAs-based MOCSER with a layer of silicon oxide reduces dramatically its sensitivity due to eliminating the ability to modify the surface states on the GaAs (see below). This reduction in sensitivity was not observed when the device was coated with MPS.

Membrane Formation on MPS-Coated GaAs Devices. The bilayer membrane was formed on the MPS-coated GaAs devices by the vesicle fusion method.[41−43] Egg phosphatidylcholin (EPC), 1,2-dioleoyl-*sn*-glycero-3-phosphoethanolamine-N-(lissamine rhodamine B sulfonyl) (LRBPE), and 1,2-dioleoyl-*sn*-glycero-3-phosphoethanolamine-N-(cap biotinyl) (BCPE) were the lipids used in this study.

Vesicles were prepared according to a protocol described by Barenholz et al.[44] and Boukobza et al.[45] Individual EPC lipids or mixtures of EPC−LRBPE (99:1 molar ratio) or mixtures of EPC−BCPE (8:2 molar ratio) were first diluted in *tert*-butyl alcohol and then lyophilized to remove all traces of organic solvent. The dry phospholipids were rehydrated by phosphate buffer, creating multilamellar vesicles. Unilamellar vesicles were formed by sonication followed by repetitive extrusion through polycarbonate films to form either 100 or 50 nm vesicles. Vesicle size distribution was measured using dynamic light scattering, and was found to be about 10% in a typical preparation (see Supporting Information for the details). Although vesicles were found to be stable for several days in 0.05 M phosphate buffer, pH 7.0, in the present work all vesicles were used immediately after preparation.

The characterization of the membrane formation was performed on GaAs substrate and not on the device itself. In order to ensure the adhesion of the bilayer membrane, (3-aminopropyl)-trimthoxysilane (APS) was adsorbed on top of the MPS-coated GaAs samples and GaAs/AlGaAs devices by overnight evaporation inside a sealed Petri dish at room temperature. Solutions containing 50 nm or 100 nm EPC vesicles, mixtures of 50 nm or 100 nm EPC−LRBPE (99:1) vesicles, or mixtures of 50 nm EPC−BCPE (8:2) vesicles were injected into a flow cell constructed on either MPS−APS-coated GaAs substrate or MPS−APS-coated MOCSER devices. The mixtures of vesicles were introduced into the flow cell either manually or using a peristaltic pump

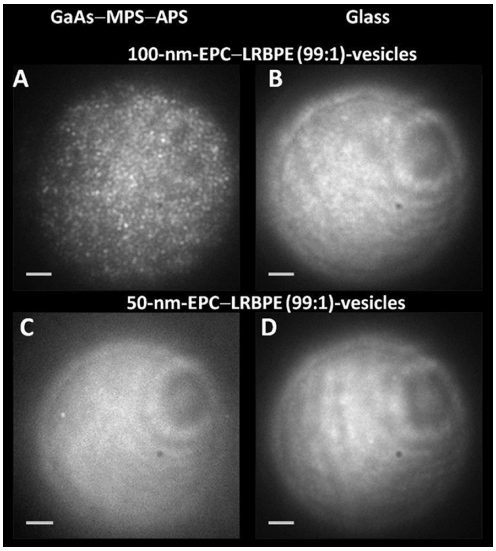

Figure 3. Fluorescence images of a GaAs surface (coated with MPS-APS) and a glass slide (etched in HF) after exposure to 50 nm and 100 nm EPC−LRBPE (99:1) vesicles and incubation for 5 min. (A) Indication for unruptured vesicles observed on the MPS−APS-coated GaAs substrates when 100 nm EPC−LRBPE (99:1) vesicles were used. (B) The same vesicles formed a bilayer membrane on a glass slide, manifested as a much more uniform fluorescence distribution. Using smaller EPC−LRBPE (99:1) vesicles (50 nm) leads to a uniform bilayer membrane formation on both MPS−APS-coated GaAs substrates (C) and glass slides (D). Scale bar: 35 μm.

operating at a flow rate of 0.02 mL/min. After injecting the vesicles, they were incubated for various times (from 5 min to 24 h) in order to undergo fusion and spread on the surface. The samples were then rinsed with phosphate buffer to remove unfused lipid excess. For comparison, bilayer membranes were constructed also on a hydrogen-fluoride-etched glass slide (see Supporting Information for details).

The smoothness and integrity of the supported bilayer formed were probed both by AFM and by fluorescence microscopy, using 50 nm or 100 nm EPC−LRBPE (99:1) vesicles. AFM images of the lipid bilayers were acquired by "gentle" tapping mode in 0.05 M phosphate buffer solution, pH 7.0 at room temperature (23−25 °C). The "gentle" tapping was applied to avoid a possible damage to the membranes and influence of the scanning itself on the membrane state.

Fluorescence imaging of the obtained bilayers indicates that in order to obtain the homogeneous surface coverage of the MPS−APS-modified GaAs substrates 50 nm vesicles should be used (see Figure 3A

dx.doi.org/10.1021/la203502b |*Langmuir* 2012, 28, 1020–1028

and C). This is in contrast to the case of hydrogen fluoride etched glass slide where 100 nm vesicle size is enough for uniform membrane formation (Figure 3B and D). The surfaces were illuminated with 532 nm light. It is well-known that unilamellar lipid vesicles can fuse and spread on surfaces such as glass to form homogeneous surface coverage of a lipid bilayer.[45] Hence, we could compare the results on glass with those on MPS-coated GaAs substrate. When the vesicles on the surface were unruptured, the fluorescence image was non-homogeneous and looked grainy (Figure 3A). The image looks smooth when the sample is illuminated with a 532 nm beam in the absence of the vesicles. It was found that incubation time of 5 min of the EPC−LRBPE (99:1) vesicles on the MPS−APS-coated GaAs substrate was sufficient for vesicle adhesion and rupture into a bilayer membrane. However, some vesicles remained unruptured, leading to a grainy fluorescence image. Longer incubation time prior to washing with phosphate buffer increases the number of the unruptured vesicles (see Supporting Information Figure S1). Downsizing the EPC−LRBPE (99:1) vesicles from 100 to 50 nm decreases dramatically the number of unruptured vesicles on the MPS−APS-coated GaAs substrate, leading to a similar homogeneous image as observed on a hydrogen fluoride etched glass slide (Figure 3C). The membrane attachment to the MPS-coated GaAs devices improves in the presence of APS relative to a membrane attachment in the absence of APS (data not shown).

The effect of vesicle size on the formation of a homogeneous bilayer on the MPS−APS-coated MOCSER substrate was evaluated also with AFM (see Supporting Information, Figure S2). The root-mean-square roughness value of the ∼25 nm MPS−APS-coated GaAs devices was found to be ∼1.6 nm. The MPS polymer was not homogeneous and contained some holes which varied from 5 to 120 nm in diameter, sufficient to trap a single 100 nm vesicle, subsequently preventing its attachment to nearby vesicles and rupture. By downsizing the vesicles size from 100 to 50 nm, the possibility of two vesicles to adsorb to the same hole was increased, subsequently leading to their rupture into a homogeneous bilayer due to sufficient surface density of vesicles.[41]

The stability and integrity of membrane formed on MPS−APS-coated GaAs substrate over time were compared to the stability and integrity of membrane formed on glass, using fluorescence imaging. While the membrane adsorbed on glass was stable for more than 7 days in the presence of 2 mM $CaCl_2$, the integrity of membrane adsorbed on MPS−APS-coated GaAs substrate deteriorated after ∼5 days (data not shown).

The results presented here and in the Supporting Information prove that indeed the GaAs device can be coated with a protecting layer of MPS and that a uniform membrane can be formed on top of an APS-MPS coated device.

Streptavidin Attachment to the EPC-BCPE (8:2) Membranes. After formation of a supported membrane of the 50 nm EPC-BCPE (8:2) vesicles on the MPS−APS-covered MOCSER devices, avidin or streptavidin solutions were added and allowed to interact with the biotin molecules for 5 min prior to washing with 0.05 M of phosphate buffer, pH 7.0. In some experiments, 50 nm EPC-BCPE(498:1) vesicles were added and allowed to interact for 5 min with the surface-adsorbed streptavidin molecules prior to washing with 0.05 M of phosphate buffer, pH 7.0. Streptavidin attachment to EPC-BCPE (8:2) membranes was confirmed by AFM (see Supporting Information Figure S3).

Measurements Procedure. The PDMS-based-microfluidic device, shown in Figure 1A, contained a flow channel (4 mm length and width and 0.6 mm in height) that was placed on top of the sensing compartment and glued with epoxy in order to localize the solvent above the MOCSER devices. To prevent damage to the supported bilayer, the MOCSER devices were kept in liquid medium during the measurements. Analytes were dissolved in the phosphate buffer and were injected sequentially into the flow cell. Phosphate buffer solution was injected sequentially between analytes to rinse the sensing area. The signal measured during this time was used as a baseline in the data analysis. Phosphate buffer (0.05 M pH 7.0) was used in all the experiments except the case of monoclonal mouse antistreptavidin antibody where phosphate buffer 0.05 M pH 7.4 was used.

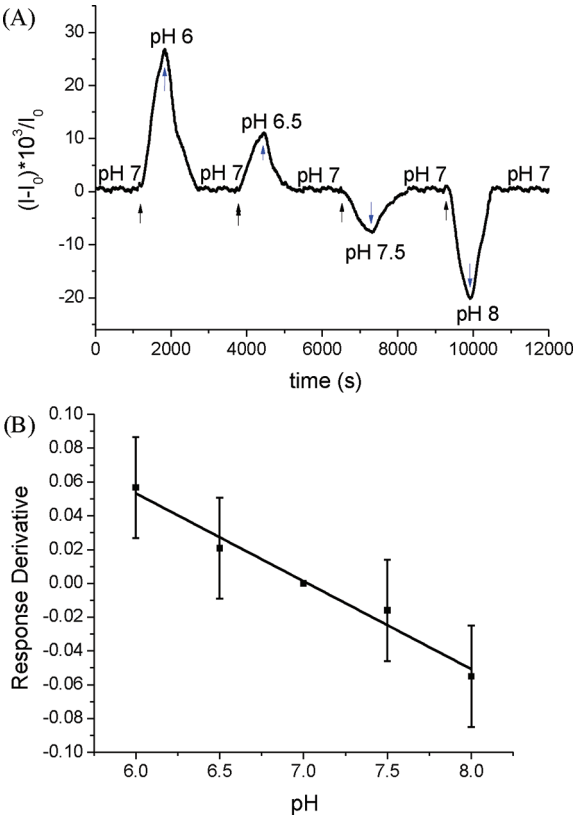

Figure 4. (A) Normalized change in the MOCSER source−drain current as a function of time when sequentially exposing the EPC-based membrane adsorbed on the device to a 0.05 M phosphate buffer solution at a pH ranging from pH 6.0 to pH 8.0 under a laminar flow of 0.02 mL/min. The black arrows indicate the time when the device was exposed to the solution with the pH indicated in the graph. The blue arrows indicate the exposing of the device to a solution with pH = 7. (B) Normalized response curve based on the derivative (slope) of the change in the signal in the peaks' half-maximum for different pH solutions.

A voltage of 1.0 V was applied between source and drain, and the change in source−drain current was monitored as a function of time. An Ag/AgCl reference electrode was used to provide a stable reference potential in the solution. It was placed in a sealed tube, connected to the main reaction compartment via a salt bridge. All measurements were performed using four MOCER devices simultaneously.

RESULTS AND DISCUSSION

Response to Various Analytes. Figure 4 presents the change in the current through the MOCSER when the device is exposed to phosphate buffer solutions with pH ranging from pH 6.0 to pH 8.0. Following the time it takes the solution to reach the sensor, the MOCSER source−drain current response to pH change is immediate and stable. The response of the device to pH is linear within the range studied (Figure 4B).

Changes in the source−drain current of the membrane-coated MOCSER device were observed when it was exposed to various concentrations of negatively or positively charged amino acids at pH = 7, exemplified by L-glutamic acid (Figure 5A) or L-lysine (Figure 6A), respectively. The MOCSER source−drain current response is correlated with the concentration of the analyte

dx.doi.org/10.1021/la203502b |Langmuir 2012, 28, 1020–1028

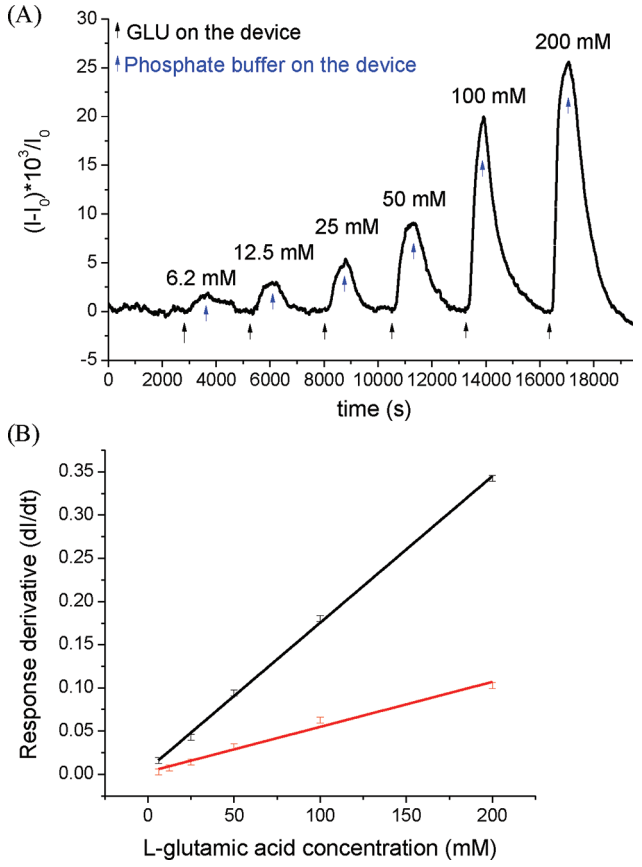

Figure 5. (A) Normalized change in MOCSER source−drain current as a function of time when the membrane-coated GaAs devices were exposed to L-glutamic acid. A rapid increase in current was observed (black arrows) upon injection of the L-glutamic acid. The current decreased when the L-glutamic acid was washed out by phosphate buffer (blue arrows). (B) Plot of the change in the normalized current (the derivative of the signal) using either MPS−APS-coated GaAs devices (black) or devices covered additionally by an EPC membrane (red).

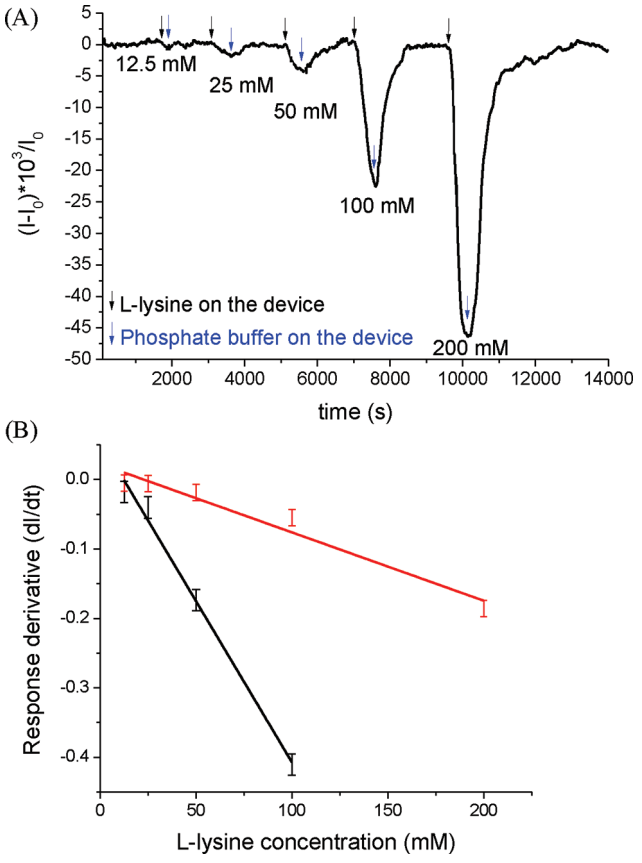

Figure 6. (A) Normalized change in MOCSER source−drain current as a function of time when the membrane-coated GaAs devices were exposed to L-lysine. A rapid decrease in current observed in the presence of L-lysine (black arrows). The current increased when the L-lysine was washed out by phosphate buffer (blue arrows). (B) Plot of the change in the normalized current (the derivative of the signal) in case of the MPS−APS-coated GaAs devices (black) and the devices covered by EPC membrane (red).

molecules. While the current increased as the concentration of L-glutamic acid increased, it decreased with increasing L-lysine concentration. The calibration plots are obtained by plotting the derivative of the signal as a function of time versus the analyte concentration (Figure 5B and Figure 6B). The change in the signal upon exposing the sensor to the analytes depends on the flow rate in the microfluidic device, on the specific response of the MOCSER to the analyte, and on the analyte concentration. Since the flow rate was maintained constant through all the measurements and the only parameter that was varied was the analyte concentration, the derivative of the signal should be proportional to the concentration of the analyte. Indeed, the signal derivative, as measured at about 200 s after exposure to the solution, was found to be proportional to the concentration of the analyte. Monitoring the gradient instead of the maximum current ensures better reproducibility of the signal and eliminates contribution from baseline shift.

The detection thresholds for L-lysine and L-glutamic acid in the presence of EPC membrane were about 12.5 mM and 6.2 mM, respectively. The detection thresholds improved to 3.2 mM and 1.6 mM for L-lysine and L-glutamic acid, respectively, in the absence of the membrane. These data further confirm the existence of the membrane on the MOCSER. Clearly, the membrane reduces the sensitivity of the device by about a factor of 4.

It is interesting to note that while the change in the signal, in the case of the pH measurements, is proportional to the logarithmic change in the concentration of the protons, it is almost linearly dependent on the concentration of the amino acids. This phenomenon is not related to the existence of the membrane and hence indicates that there is a different mechanism for the effect of both types of species (protons and organic acids) on the MOCSER.

For detecting streptavidin and rabbit antistreptavidin antibodies, we used the strategy presented in Figure 7. In this case, we used an EPC−BCPE (8:2) membrane, which has a fraction of ∼20% biotin. Attachment of streptavidin to the membrane was evidenced and characterized by AFM using as a marker biotin-labeled 50 nm EPC−BCPE (498:1) vesicles (Supporting Information, Figure S3A). The 50 nm EPC−BCPE (498:1) vesicles were not observed in the absence of streptavidin (see Supporting Information, Figure S3C). Exposing the membrane to either streptavidin or avidin at concentrations above 0.8 μM at pH = 7 resulted in a significant change in the MOCSER source−drain current. The current increased upon exposure to streptavidin concentration (Figure 8A), but the signal did not recover even when the solution was changed to buffer with no streptavidin.

dx.doi.org/10.1021/la203502b |*Langmuir* 2012, 28, 1020–1028

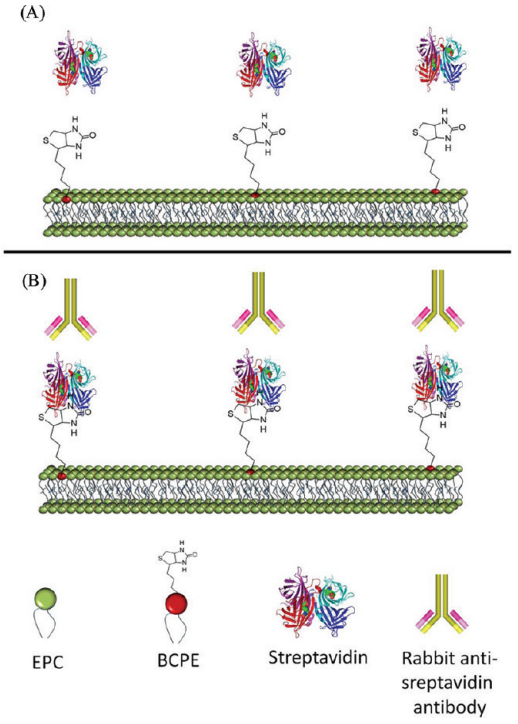

Figure 7. Schematic illustration of the strategy used for surface modification with streptavidin (A) and rabbit antistreptavidin antibody (B) for detection by the devices coated with a biotinylated membrane (EPC−BCPE (8:2)).

This result indicates strong binding of the streptavidin to the biotin which is seemingly irreversible on the time scale of the experiment. When exposed to avidin, the current through the MOCSER was reduced (Figure 8B). When a membrane without biotin (EPC-based membrane) was also exposed to the same solution, some change in current was observed, but this change was completely reversed by washing with buffer.

While streptavidin is negatively charged at neutral pH, avidin is positively charged. Hence a reverse effect on the current is observed in accordance with the observations when amino acids were probed. Hence it can be generalized that a negatively charged analyte causes an increase in the current through the MOCSER while positively charged analyte causes a decrease in the current.

Change in the MOCSER source−drain current was observed when the devices to which streptavidin was initially attached were exposed to polyclonal rabbit antistreptavidin antibody in serum (Figure 9A, right). In this case, the current decreased upon exposure to the antibodies at concentrations of 0.031, 0.125, and 1 mg/mL. Irreversible negative offset in current was observed following washing with a buffer solution indicating binding of the antistreptavidin molecules to biotin−streptavidin complex. However, when the serum contained no antibodies, the signal returned to the baseline upon washing (Figure 9A, left). The fact that the signal is not returning to the baseline, when the antibodies are present, reflects the strong binding of the antibody to the streptavidin. As a control experiment, devices with no biotin (EPC-based membrane) and hence no bound streptavidin were exposed to the same serum solution that contained the antibody. A small positive offset in current was observed upon washing indicating nonspecific binding of serum species to the membrane. The normalized response of the current is plotted in Figure 9C as a function of the amount of antibodies to which they

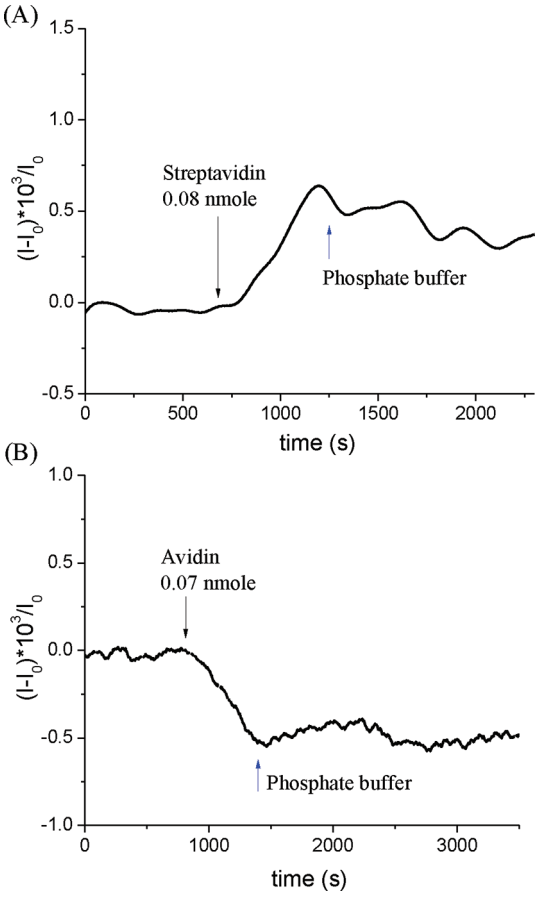

Figure 8. Response of a MOCSER device coated with a biotin-containing membrane EPC−BCPE (8:2) upon exposure to streptavidin (A) and avidin (B) molecules. In both cases, the indicated amount of material was dissolved in 100 μL.

were exposed. The amount of analyte is presented (and not the concentration) since the binding of the analyte is seemingly irreversible and the signal is accumulating as a function of the amount of analyte to which the sensor is exposed. The two curves relate to devices coated with biotinylated membrane (EPC−BCPE (8:2) based membrane) to which streptavidin was attached (black curve) and to devices coated with a membrane without biotin (EPC-based membrane, blue curve).

For comparison, Figure 9B shows the normalized change in current obtained when the device was exposed to various concentrations of monoclonal mouse antistreptavidin antibody. In this case, the signal increased upon exposure to the antibodies and exhibited a baseline offset upon washing with the buffer solution. The difference in the trend of the response (negative vs positive offset in Figure 9A,B, respectively) is probably due to different charge on each type of antibody. The normalized response of the current through the MOCSER due to interaction of mouse antistreptavidin antibody with streptavidin is shown in Figure 9D. Here, clearly a nonlinear response of the device to the concentration is observed. The nonlinearity in the response is not evident in other cases (Figure 9C) because of the limited range of the analyte concentrations to which the sensor was exposed and due to the low number of data points that do not allow a nonlinear fit.

Sensing Mechanism. The operation of the MOCSER as a sensor is based on it being capacitance sensitive.[46] Thus, when

dx.doi.org/10.1021/la203502b |*Langmuir* 2012, 28, 1020–1028

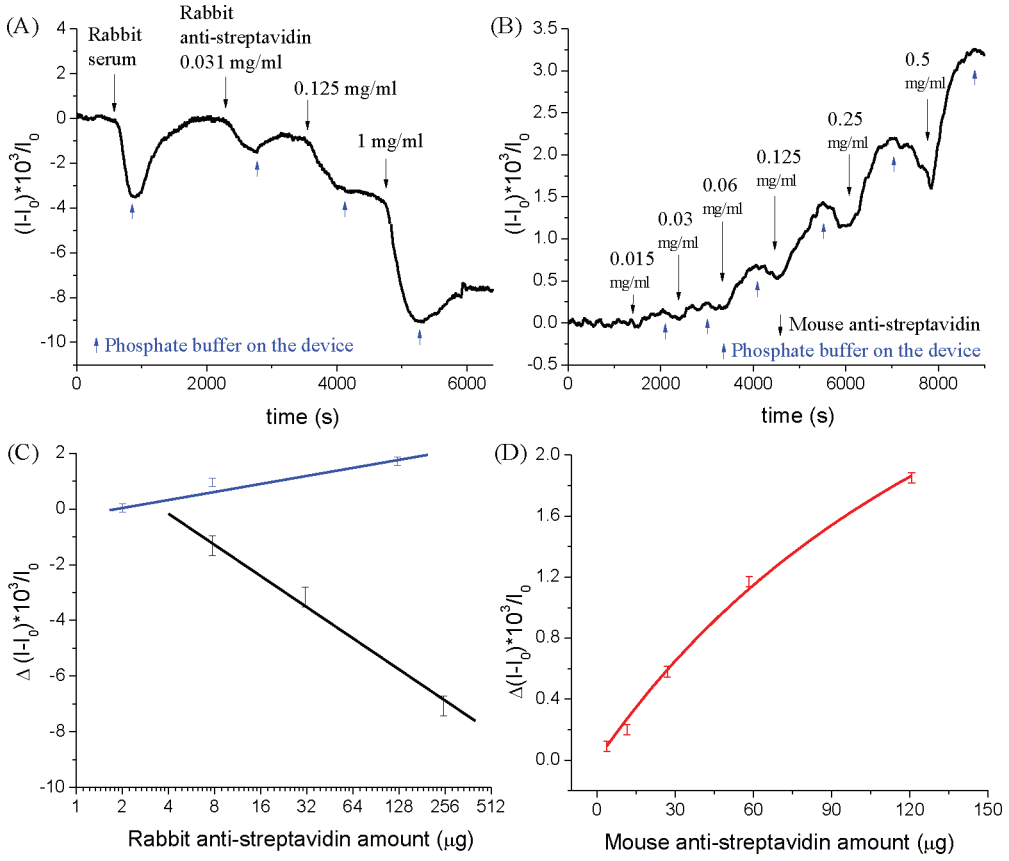

Figure 9. (A) Normalized change in the MOCSER source−drain current as a function of time when exposed to rabbit antistreptavidin antibody (whole antiserum) and rabbit serum alone (no antibodies). After exposure to serum, the signal recovers to the baseline when rinsing with the phosphate buffer, while there is a nonreversible baseline offset in case of exposure to the rabbit antistreptavidin antibody solution, resulting from specific interaction between immobilized streptavidin and rabbit antistreptavidine antibodies. (B) Normalized change in current when the device is exposed to different concentrations of mouse antistreptavidin antibody (purified). In this case, the signal exhibits nonreversible baseline offset upon washing with the buffer solution. (C) Calibration curve for response due to strong interaction of rabbit antistreptavidin antbody with streptavidin (black), compared to the weak interaction of the same antibodies with nonbiotinylated membrane (blue). (D) Calibration curve for response due to interaction of mouse antistreptavidin antibody with streptavidin.

the device is immersed in electrolyte solution with a reference electrode, a double layer is formed on its surface (see Figure 10). Clearly, when the analyte on the surface of the membrane is negatively charged, the charge accumulating on the surface of the device is positive and vice versa. Since the device is based on n-doped GaAs, positive charge on the surface increases the charge carrier concentration in the conductive channel and the source−drain current increases. The opposite is true for negative charge on the surface of the GaAs that causes depletion in the charge carrier concentration and hence reduction in the source−drain current.

The amount of charge accumulating on the surface of the GaAs per charge on the analyte depends on the potential, V, built between the surface of the membrane and the GaAs surface which is given by $V \propto Qd/\varepsilon$, where Q is the charge per surface area of the analyte, d is the thickness of the MPS−APS−membrane layer, and $\varepsilon \approx 2$ is the electric permittivity of this layer. Since most of the thickness is due to the MPS layer, its value is about the same for a system with or without the membrane. Hence, the difference between the response curves obtained with and without a membrane (Figure 5B and Figure 6B) stems from increase of ε upon coating the device with the membrane. This increase can be due to a thin water layer located between the membrane and the APS layer.

The MOCSER is different from the well-developed ion-selective FET (ISFET)[47,48] where the gate on the transistor is replaced with ion-selective membrane that allows specific ions to penetrate, and these ions define the electric potential on the gate. It is also different from the regular CHEMFET or IGFET where the metal gate terminal is coated with molecules that interact with a specific analyte.[49] In these cases, the detection is performed by monitoring the change in the gate potential required for maintaining a constant current.

In the present device, the current through the device for a given source−drain potential is determined by the resistivity which is controlled by the band bending in the semiconductor: the more bent the bands, the lower the current. In general, the band bending is determined by the charge on the surface states. Hence, the sensitivity of the device stems from the change induced in the surface states charge. The density of surface states of GaAs is of about 10^{13} states/cm^2, and it has been shown that a change of about 1% in this charge is enough to affect in a detectable way the current.[10] The dipole moment that would result from this charge reorganization would have very little effect on the surface potential and would not be felt by the MOCSER.[24] Hence, the surface states are the source of sensitivity of the current sensor, a sensitivity exceeding what can be obtained by modifying the voltage on a metal gate.

The work presented here demonstrates the sensing of various species that interact differently with the membrane-coated MOCSER.

dx.doi.org/10.1021/la203502b |*Langmuir* 2012, 28, 1020–1028

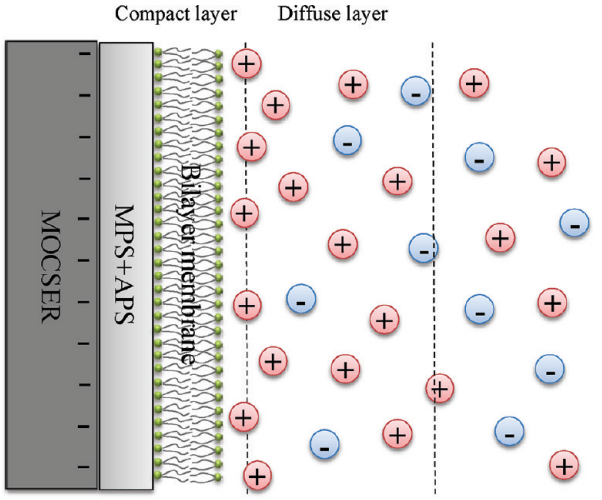

Figure 10. Scheme of the double layer formed on the surface of the MOCSER. The MPS layer is not in scale, and in reality, it is about a hundred times thicker than the membrane. In the case of high concentration of cations in the double layer, the MOCSER surface is negatively charged and the current decreases, while for high anion concentration, the surface becomes positively charged and the current through the MOCSER increases.

In the case of pH and amino acid sensing, the interaction of the analytes with the substrate is weak, as validated by the ability to remove the analyte from the sensor by washing with the buffer solution. The dependence of the signal on the analyte concentration in these cases is complicated, because it reflects the change in the double layer charge and the extent that this change affects the charge on the MOCSER surface itself. It is important to realize that, since the molecules forming the membrane are zwitterions, no preference, in terms of the interaction strength, is observed in the two oppositely charged amino acids.

When the analytes interact strongly with the biotin-containing membrane, the signal is irreversible on the time scale of the measurement, but depends on the charge of the analytes in the same manner as in the case of nonspecific weak interactions.

The approach presented here, in which chemical interaction, occurring on the outer side of the membrane, is transformed into an electric signal which is sensed at the interior membrane side using a MOCSER, can be implemented for studying protein−membrane and protein−protein interactions and kinetics. In principle, proteins can also be incorporated within the membrane, which should ensure a correct conformation and facilitate sensing their interactions with molecules in solution. The sensitivity of the system presented here is not reaching that obtained by fluorescence methods, despite the very high sensitivity observed in past gas-phase measurements with the MOCSER.[37] This low sensitivity results from combination of parameters that were not optimized in the present study, like the dimensions of the MOCSER device itself, the thickness of the APS layer, and the measuring setup. Hence, there is a wide range of parameters that can be improved for the device to reach much higher sensitivity. However, the uniqueness of the present setup is the ability to conduct direct electrical measurements on a micrometer-sized device. This feature singles out the technique as compared to other available methods and may allow development of an in vivo measuring system.

■ ASSOCIATED CONTENT

Supporting Information. Detailed experimental procedures, list of analytes and chemical used, and measuring conditions. It also includes fluorescence images of vesicles on MPS-APS-coated GaAs substrate. This material is available free of charge via the Internet at http://pubs.acs.org.

■ AUTHOR INFORMATION

Author Contributions

[§]The first two authors contributed equally.

■ ACKNOWLEDGMENT

The authors thank Dr. Arkady Bitler from the Chemical Research Support for his help with the AFM measurements. R.N. acknowledges the support of the Grand Center for Sensors and Security. This work was supported by the NaBi CNRS-Weizmann collaboration.

■ REFERENCES

(1) See, for example:Chattopadhyay, A.; Raghuraman, H. *Curr. Sci.* **2004**, *87*, 175–180.
(2) Baciu, C. L.; Becker, J.; Janshoff, A.; Sönnichsen, C. *Nano Lett.* **2008**, *8*, 1724–1728.
(3) Thompson, M.; Krull, U. J. *Anal. Chim. Acta* **1982**, *141*, 33–47.
(4) Thompson, M.; Krull, U. J.; Bendell-Young, L. I. *Talanta* **1983**, *30*, 919–924.
(5) Umezawa, Y.; Kataoka, M.; Takami, W. *Anal. Chem.* **1988**, *60*, 2392–2396.
(6) Woodhouse, G.; King, L.; Wieczorek, L.; Osman, P.; Cornell, B. *J. Mol. Recognit.* **1999**, *12*, 328–334.
(7) Xu, Y.; Bakker, E. *Langmuir* **2009**, *25*, 568–573.
(8) Dumas, C.; Zein, R. E.; Dallaporta, H.; Charrier, M. *Langmuir* **2011**, *27*, 13643–13647.
(9) Coldrick, Z.; Penezić, A.; Gašparović, B.; Steenson, P.; Merrifield, J.; Nelson, A. *J. Appl. Electrochem.* **2011**, *41*, 939–949.
(10) Capua, E.; Natan, A.; Kronik, L.; Naaman, R. *ACS Appl. Mater. Interfaces* **2009**, *1*, 2679–2683.
(11) Eeman, M.; Deleu, M. *Biotechnol. Agron. Soc. Environ.* **2010**, *14*, 719–736.
(12) Mueller, P.; Rudin, D. O.; Tien, H. T; Wescott, W. C. *Circulation* **1962**, *26*, 1167–1171.
(13) Del Castillo, J.; Rodriguez, A.; Romero, C. A.; Sanchez, V. *Science* **1966**, *153*, 185–188.
(14) Tanaka, M.; Sackmann, E. *Nature* **2005**, *437*, 656–663.
(15) Bieri, C.; Ernst, O. P.; Heyse, S.; Hofmann, K. P.; Vogel, H. *Nat. Biotechnol.* **1999**, *17*, 1105–1108.
(16) Sackmann, E.; Tanaka, M. *Trends Biotechnol.* **2000**, *18*, 58–64.
(17) Sapuri, A. R.; Baksh, M. M.; Groves, J. T. *Langmuir* **2003**, *19*, 1606–1610.
(18) Yip, C. M.; Darabie, A. A.; McLaurin, J. *J. Mol. Biol.* **2002**, *318*, 97–107.
(19) Poghossian, A.; Abouzar, M. H.; Amberger, F.; Mayer, D.; Han, Y.; Ingebrandt, S.; Offenhäusser, A.; Schöning, M. J. *Biosens. Bioelectron.* **2007**, *22*, 2100–2107.
(20) Chai, L.; Cahen, D. *Mater. Sci. Eng., C* **2002**, *19*, 339–343.
(21) Cahen, D.; Naaman, R.; Vager, Z. *Adv. Funct. Mater.* **2005**, *15*, 1571–1578.
(22) Vilan, A.; Cahen, D. *Trends Biotechnol.* **2002**, *20*, 22–29.
(23) Cohen, R.; Bastide, S.; Cahen, D.; Libman, J.; Shanzer, A.; Rosenwaks, Y. *Opt. Mater.* **1998**, *9*, 394–400.
(24) Naaman, R. *Phys. Chem. Chem. Phys.* **2011**, *13*, 13153–13161.
(25) Bergveld, P. *IEEE Trans. Biomed. Eng.* **1972**, *19*, 342–351.

(26) Bergveld, P.; DeRooij, N. F.; Zemel, J. N. *Nature* **1978**, *273*, 438–443.
(27) Thévenot, D. R.; Toth, K.; Durst, R. A.; Wilson, G. S. *Biosens. Bioelectron.* **2001**, *16*, 121–131.
(28) Baumann, W. H.; Lehmann, M.; Schwinde, A.; Ehret, R.; Brischwein, M.; Wolf, B. *Sens. Actuators, B* **1999**, *55*, 77–89.
(29) Kharitonov, A. B.; Zayats, M.; Lichtenstein, A.; Katz, E.; Willner, I. *Sens. Actuators, B* **2000**, *70*, 222–231.
(30) Schöning, M. J.; Poghossian, A. *Analyst* **2002**, *127*, 1137–1151.
(31) Bergveld, P. *Sens. Actuators, B* **2003**, *88*, 1–20.
(32) Janata, J. *Electroanalysis* **2004**, *16*, 1831–1835.
(33) Goykhman, I.; Korbakov, N.; Bartic, C.; Borghs, G.; Spira, M. E.; Shappir, J.; Yitzchaik, S. *J. Am. Chem. Soc.* **2009**, *131*, 4788–4794.
(34) Gartsman, K.; Cahen, D.; Kadyshevitch, A.; Libman, J.; Moav, T.; Naaman, R.; Shanzer, A.; Umansky, V.; Vilan, A. *Chem. Phys. Lett.* **1998**, *283*, 301–306.
(35) Vilan, A.; Ussyshkin, R.; Gartsman, K.; Cahen, D.; Naaman, R.; Shanzer, A. *J. Phys. Chem. B* **1998**, *102*, 3307–3309.
(36) Capua, E.; Cao, R.; Sukenik, C. N.; Naaman, R. *Sens. Actuators, B* **2009**, *140*, 122–127.
(37) Rei Vilar, M.; El-Beghdadi, J.; Debontridder, F.; Naaman, R.; Arbel, A.; Ferraria, A. M.; Botelho Do Rego, A. M. *Mater. Sci. Eng., C* **2006**, *26*, 253–259.
(38) Rudich, Y.; Benjamin, I.; Naaman, R.; Thomas, E.; Trakhtenberg, S.; Ussyshkin, R. *J. Phys. Chem. A* **2000**, *104*, 5238–5245.
(39) Wu, D. G.; Cahen, D.; Graf, P.; Naaman, R.; Nitzan, A.; Shvarts, D. *Chem.—Eur. J.* **2001**, *7*, 1743–1749.
(40) Kirchner, C.; George, M.; Stein, B.; Parak, W. J.; Gaub, H. E.; Seitz, M. *Adv. Funct. Mater.* **2002**, *12*, 266–276.
(41) Richter, R. P.; Bérat, R.; Brisson, A. R. *Langmuir* **2006**, *22*, 3497–3505.
(42) Wong, J. Y.; Majewski, J.; Seitz, M.; Park, C. K.; Israelachvili, J. N.; Smith, G. S. *Biophys. J.* **1999**, *77*, 1445–1457.
(43) Sackmann, E. *Science* **1996**, *271*, 43–48.
(44) Barenholz, Y.; Gibbes, D.; Litman, B. J.; Goll, J.; Thompson, T. E.; Carlson, F. D. *Biochemistry* **1977**, *16*, 2806–2810.
(45) Boukobza, E.; Sonnenfeld, A.; Haran, G. *J. Phys. Chem. B* **2001**, *105*, 12165–12170.
(46) Ghafar-Zadeh, E.; Sawan, M.; Chodavarapu, P. V.; Hosseini-Nia, T. *IEEE Trans. Biomed. Circuits Syst.* **2010**, *4*, 232–238.
(47) McKinley, B. A.; Houtchens, B. A.; Janata, J. *Ion-Sel. Electrode Rev.* **1984**, *6*, 173–208.
(48) Fogt., E. J.; Untereker, D. F.; Norenberg, M. S. *Anal. Chem.* **1985**, *57*, 1995–1998.
(49) Lee, C. S.; Kim, S. K.; Kim, M. *Sensors* **2009**, *9*, 7111–7131.

■ NOTE ADDED AFTER ASAP PUBLICATION

This article was published ASAP on December 14, 2011. Figures 4, 5, 6, and 8 have been modified. The correct version was published on December 21, 2011.